Self-Association and Backbone Dynamics of the Hck SH2 Domain in the Free and Phosphopeptide-Complexed Forms†

Weixing Zhang,‡ Thomas E. Smithgall, and William H. Gmeiner*

The Eppley Institute for Research in Cancer and Allied Diseases, The University of Nebraska Medical Center, Omaha, Nebraska 68198-6805

Received August 21, 1997; Revised Manuscript Received February 25, 1998

ABSTRACT: Decreased dynamic motion in the peptide backbone of proteins may accompany ligand binding and influence the thermodynamic and kinetic stability of the resulting complexes. We have investigated the diffusional behavior and backbone dynamics of the free and phosphopeptide (EPQpYEEIPIYL) complexed Hck SH2 domain using NMR spectroscopy. Both the free domain and its phosphopeptide complex self-associate at higher protein concentrations. Diffusional measurements and surface analysis indicate that charged side-chain groups are probably responsible for self-association. Higher order aggregation, such as trimer and tetramer, also occurs at elevated protein concentrations. Dynamic motion in the peptide backbone of Hck SH2 was determined from ^{15}N relaxation data fit using extended model-free parameters. The rotational correlation time (τ_m) for uncomplexed Hck SH2 was 6.8 ns while τ_m for peptide-bound Hck SH2 was 7.6 ns. Generalized order parameters (S^2) increased for most residues upon binding of the phosphopeptide, consistent with peptide binding restricting motion of the NH bond vectors on the picosecond time scale. These studies suggest that complexation increases internal order in Hck SH2 and that internal dynamic motions contribute to the activation of Src-family kinases in vivo.

The SH2 domain is a protein module of approximately 100 amino acid residues that occurs frequently in proteins involved in intracellular signal transduction, including the Src-family protein tyrosine kinases (PTKs)[1] (*1*, *2*). The prototypical SH2 domain fold consists of three central β-sheets and two α-helices, which pack on either side of it. This fold results in two binding pockets on the SH2 domain surface which bind phosphotyrosine and a hydrophobic side chain (frequently Leu or Ile), respectively. The SH2:ligand interaction thus resembles a "two-pronged plug" engaging a "two-holed socket" (*3*).

In the context of the Src family of nonreceptor protein-tyrosine kinases, SH2 domains contribute to the negative regulation of kinase activity. Phosphorylation of a highly conserved tyrosine residue in the tail region induces intramolecular interaction with the SH2 domain, contributing to the stabilization of an inactive conformation for the kinase. The tail residue is phosphorylated by a distinct regulatory kinase known as Csk (*4*). The inactive form of Src is stabilized by an additional intramolecular interaction between the SH3 domain and a polyproline type II helix formed by the linker connecting the SH2 and kinase domains. The latter interaction was discovered only recently with the solution of high-resolution X-ray structures of the inactive, tail-phosphorylated forms of c-Src and Hck (*5*, *6*). A growing body of literature shows that SH2- or SH3-mediated binding to other proteins induces Src family kinase activation, presumably by displacing one or both of the intramolecular, negative-regulatory interactions (*7*−*9*).

The hematopoietic cellular kinase (Hck) is an Src-family member that is expressed predominantly in myeloid cells of the granulocytic and monocytic lineages (*10*−*13*). Hck is rapidly induced in response to macrophage activation and has been implicated in multiple signaling events, including Fc and cytokine receptor signal transduction, integrin activation, and TNF release (*14*−*20*). Hck binds tightly to HIV Nef via its SH3 domain, and interaction of Hck with other proteins via SH2 and/or SH3 may activate Hck by disturbing the closed, inactive state (*21*−*23*).

Knowledge concerning changes in dynamic motion of the peptide backbone that accompany ligand binding are important for understanding the physicochemical basis for interaction at a molecular level (*24*−*30*). Our laboratory recently solved the structure of the SH2 domain for Hck using NMR spectroscopy (*31*; Figure 1). In this paper, we describe the diffusional behavior and the backbone dynamics of the isolated Hck SH2 domain both in the free and phosphopeptide-complexed forms. These studies are consistent with complexation of Hck SH2 resulting in a more ordered structure implying that ligand release is entropically favored by increased internal motion in the SH2 domain.

† This work was supported by NIH Grant RO1 CA58667 (T.E.S.), NIH Grant R29 60612 (WH.G.), NIH Grant P30 CA36727 (W.H.G.), and the Nebraska Department of Health.

* Corresponding author. Fax: (402) 559-4651. E-mail: bgmeiner@unmc.edu.

‡ Present address: Department of Structural Biology, St. Jude Children's Research Hospital, Memphis, TN 38105.

[1] Abbreviations: Hck, hematopoietic cellular kinase; SH, Src homology region; PTK, protein-tyrosine kinase; IL-3, interleukin-3; IL-4, interleukin-4; IL-6, interleukin-6; LIF, leukemia inhibitory factor; GM-CSF, granulocyte-macrophage colony-stimulating factor; PTB, phosphotyrosine binding domain; NMR, nuclear magnetic resonance; HSQC, heteronuclear single-quantum coherence; CSA, chemical shift anisotropy; TNF, tumor necrosis factor.

S0006-2960(97)02077-1 CCC: $15.00
Published on Web 04/29/1998

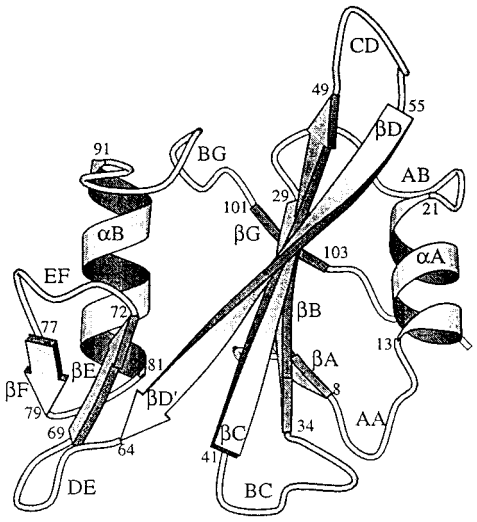

FIGURE 1: Ribbon diagram of the 3D solution structure of the Hck SH2 domain (*31*). The primary sequence is numbered such that the N-terminal methionine from bacterial expression is residue 1 and the highly conserved tryptophan is residue 6. The figure was generated using the program Molscript (*56*).

MATERIALS AND METHODS

Sample Preparation. The Hck SH2 domain (residues E119-K224 of human Hck, 12.2 kDa) was expressed and purified as described previously (*32*). The NMR sample was prepared in 90% H_2O/10% D_2O containing 100 mM NaCl, 5 mM DTT-d_{10}, and 50 mM sodium phosphate at pH 6.4. For preparation of the phosphopeptide complex (13.7 kDa), quantitative HPLC-purified phosphopeptide (AcNH-EPQpY-EEIPIYL-COOH, sequence from hamster middle T antigen) (Alberta Peptide Institute) was added to the SH2 solution to yield a slight excess of peptide relative to Hck SH2. For diffusion measurements, protein concentrations of 0.5−4.0 mM were studied, whereas the concentration for the dynamic studies was 1.0 mM for both the free and the phosphopeptide-complexed Hck SH2 domain. NMR tubes were sealed after the samples were purged with argon.

NMR Spectroscopy. All NMR experiments were performed at 28 °C using a Varian Unity 500 spectrometer equipped with a triple-resonance, pulsed-field *z*-gradient probe. NMR data were processed and analyzed using either VNMR or FELIX version 2.05 (Hare Research, Inc., Bothel, WA) using a Sparc 20 workstation. The self-diffusion coefficient was determined using a modified BPP-LED pulse sequence (*33*). Water suppression was achieved using the WET element (*34*).

The translational diffusion coefficient, *D*, is related to the observed signal intensity, *I*, through the following relationship:

$$I = I_0 \exp[-D(\gamma \delta G)^2(\Delta - \delta/3 - \tau/2)] \qquad (1)$$

where γ is the gyromagnetic ratio for protons, *G* is the gradient strength (G/cm), δ is PFG duration (s), Δ is the time between the PFG pulses (s), and τ is the gradient recovery period (s). A series of 19 spectra were acquired using different *G* values for each diffusion measurement.

The pulse sequences used to measure ^{15}N T_1, T_2, and heteronuclear NOEs were based on those described previously by Lewis E. Kay (*35, 29*). All experiments were recorded with a sweep width of 6000 Hz in the F_2 dimension and a sweep width of 1500 Hz in the F_1 dimension. A total of 128 (t_1) × 2048 (t_2) complex points were collected. A relaxation delay of 1.0 s with 16 scans/increment was used for both T_1 and T_2 experiments. The heteronuclear NOE experiments were collected with a recycle time of 5.0 and 32 scans/increment. Methods used for processing and analysis of the relaxation data are available as Supporting Information.

RESULTS AND DISCUSSION

^{1}H-^{15}N HSQC Spectra of Free and Complexed Hck SH2. The 3D solution structure of the Hck SH2 domain is presented in Figure 1 (*31*). Hck SH2 residues most affected by phosphopeptide binding were identified by comparison of ^{1}H-^{15}N HSQC spectra of a ^{15}N-enriched sample of Hck SH2 acquired in either the presence or the absence of the high affinity ligand AcNH-EPQpYEEIPIYL-COOH (K_d for Src and Lck SH2 = 3.7×10^{-9} M) (*36*). Those residues whose backbone NH chemical shifts changed significantly upon binding of the phosphopeptide are indicated in Figure 2. Large chemical shift changes were observed for several residues that have been implicated previously in complexation of this peptide with the c-Src SH2 domain (*3*). In particular, several charged residues in αA (R13, K14, and E17) and βD (H59 and K61) undergo large chemical shift changes upon complexation, consistent with positively charged residues in these secondary structural elements forming contacts with the phosphotyrosine of the ligand. The BC loop has also been implicated in binding of the high-affinity peptide, and significant complexation-induced changes in chemical shift were observed for residues in this loop (S35, E36, T37, and T38). Significant chemical shift changes were also observed for residues in those secondary structure elements implicated in contacting the Ile side chain of the high-affinity peptide in the X-ray structure of c-Src SH2. In particular, residues in the EF (I72, S73, and R75) and BG loops (G94, L95, and C96) were sensitive to complexation with the high affinity peptide. These results indicate that similar recognition motifs occur for complexation of Hck SH2 with this phosphopeptide as were observed previously for c-Src SH2 (*3*).

Self-Association of the Hck SH2 Domain. The translational diffusion coefficient for the Hck SH2 domain as a function of protein concentration was measured using the BPP-LED method (*33*). The results are presented in Figure 3. The diffusion coefficient of Hck SH2 decreased as the protein concentration was increased from 0.5 to 4.0 mM, indicating that the SH2 domain self-associates at millimolar concentrations. Concentration-dependent self-association for both free and phosphopeptide-complexed Hck SH2 suggests that residues not involved in peptide binding are responsible for the intermolecular interaction. Concentration dependent self-association has also been reported for BPTI (*37*) and the dynamin PH domain (*38*). The self-association properties of Hck SH2, however, differ from BPTI for which an apparent dissociation constant (K_d) could be obtained using a monomer−dimer equilibrium model. Attempts to fit the diffusion data for Hck SH2 to a monomer−dimer equilibrium model failed, as a global fit for the dissociation constant (K_d) could not be obtained for all protein concentrations studied

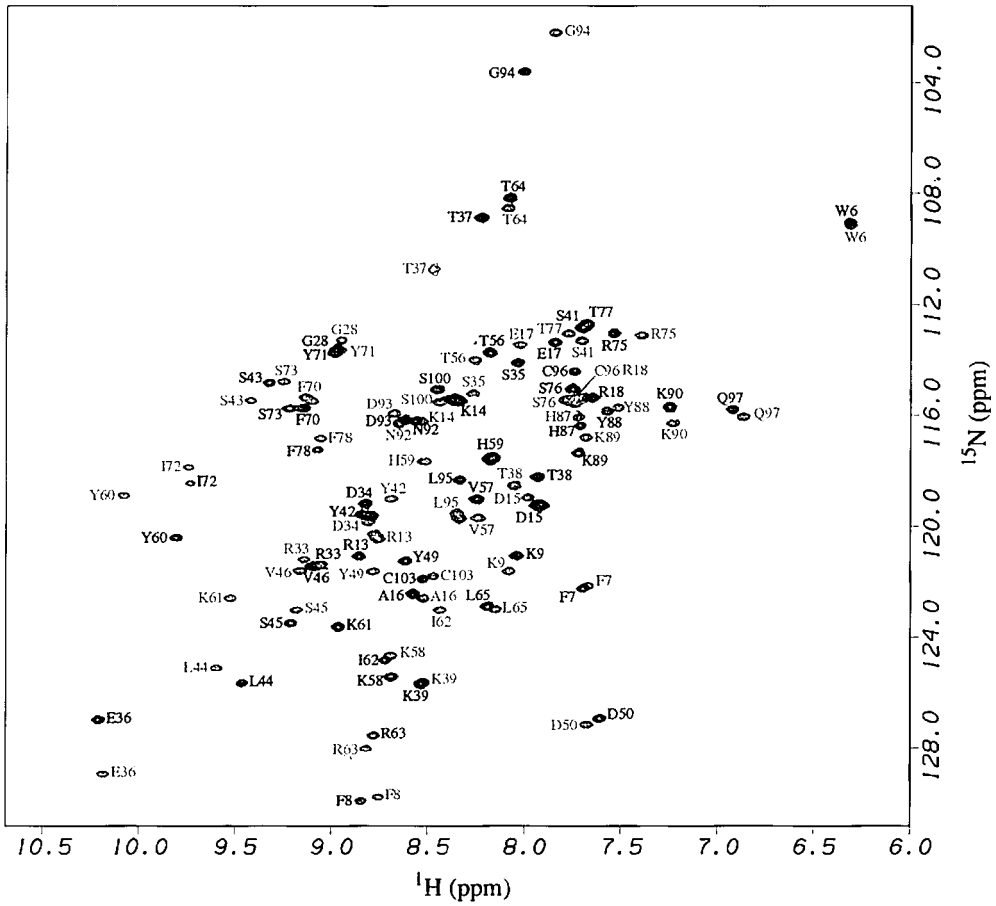

FIGURE 2: 2D ^{1}H-^{15}N HSQC spectra of the Hck SH2 domain in the free (black) and phosphopepide complexed form (red). Only those residues that show a large change in chemical shift upon binding of the phosphopeptide are shown.

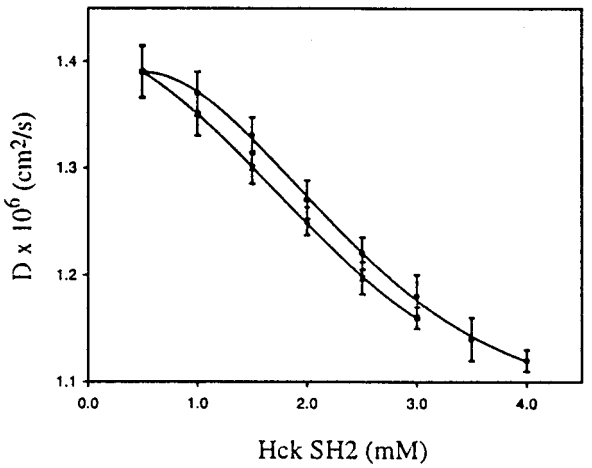

FIGURE 3: Concentration dependence of the diffusion coefficients of the Hck SH2 domain at 28 °C. The free form is shown as black dots while the phosphopeptide-complexed form is indicated as a cross

(*37*). The K_d calculated for Hck SH2 is larger at low concentrations of protein than at high concentrations (K_d = 8.4×10^{-3} M at 1 mM; 8.0×10^{-4} M at 2.5 mM). These data are consistent with aggregates of order greater than two present at higher protein concentrations.

The nature of the interaction surface for dimerization and higher order aggregation of Hck SH2 was investigated by analyzing the charge properties of solvent accessible residues. The solvent-accessible surface for each residue of uncomplexed Hck SH2 is shown in Figure 4, while the surface

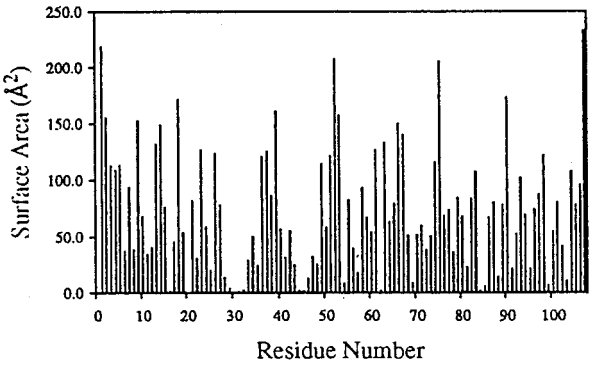

FIGURE 4: Solvent accessible surface for residues of the free Hck SH2 domain.

potential of the free Hck SH2 domain is shown in Figure 5. The phosphotyrosine binding pocket of Hck SH2 is positively charged, as expected. Only a few, noncontiguous hydrophobic residues, e.g., P23, M26, P51, P74, and M104, have relatively large solvent accessible surfaces. Conversely, many charged side chains are accessible to solvent including E2, T3, D66, and E83 for negative charges and K9, K14, R18, K39, R52, R75, and K90 for positive charges. K107 is on the C-terminus and, thus, carries both positive and negative charges. While a hydrophobic surface cannot be eliminated as one of the possibilities for the dimerization interface(s), this type of interaction surface for Hck SH2 dimerization is unlikely based on the surface potential (Figure 5).

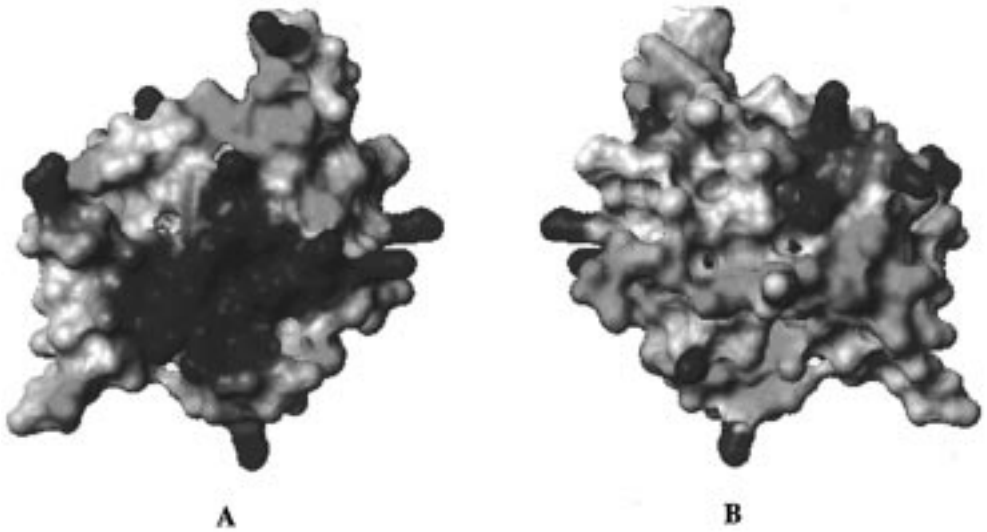

FIGURE 5: Surface potential of the free Hck SH2 domain. Negative charge is shown in red while positive charge is shown in blue. (A) The phosphotyrosine binding surface. (B) The other side of the molecule. These figures were produced using MOLMOL v2.4 (*57*).

A more likely scenario for intermolecular Hck SH2 association involves positively charged groups in one molecule of Hck SH2 interacting with negatively charged groups in another molecule providing an electrostatic basis for self-association. Consideration of rotational anisotropy for Hck SH2 from T1 and T2 relaxation studies reveals that the anisotropy of the partially aggregated species in solution is between 1.1 and 1.3, a value slightly greater than the anisotropy predicted from inertial considerations of the monomeric structure ($D_{||}/D_{\perp} = 1.28$).

Backbone Dynamics of the Free Protein. The Hck SH2 domain used in this study contains 107 residues. Among the 101 backbone amide protons (excluding the four proline residues and the two N-terminal residues which are not observed), 16 residues were excluded from the analysis due to resonance overlap. Thus, quantitative measurements were made for 85 of the amide cross-peaks. Figure 6, panels A−C, shows the relaxation data for free Hck SH2. For most residues, the T_1 values lie in the range 0.43−0.53 s (Figure 6A), and the T_2 values ranged 90−120 ms (Figure 6B). The heteronuclear NOEs for most residues were found to be in the range 0.60−0.82 (Figure 6C), indicating that internal motions on the fast (picosecond) time scale are restricted. In contrast, the two residues at the C-terminus have negative NOEs. In addition, the NOEs for T3, E4, and G69 were significantly smaller than the average.

The overall rotational correlation time, τ_m, was initially determined using the T_1 and T_2 values calculated for each residue. The optimum values of the model-free parameters S^2 and τ_e were then determined using this τ_m. The global optimum τ_m was determined considering all residues simultaneously using the previously established values of S^2 and τ_e from the grid search. The global optimum τ_m for the free Hck SH2 domain was calculated to be 6.8 ns. This value was used subsequently to determine the internal dynamics parameters.

The model-free parameters for uncomplexed Hck SH2 are shown in Figure 7, panels A−E, and summarized in Table 1. For most residues, the order parameters (S^2) were in the range 0.75−0.90, indicating that rapid motions on the fast (picosecond) time scale were largely restricted. In contrast, the order parameters (S^2) were much lower for residues T3, E4, G69, and the two residues at the N-terminus (Figure 7A). These results indicate that these segments of the protein are more mobile than the overall backbone. A significant difference in the order parameters between G69 and neighboring residues was observed indicating increased motion occurs for this residue in the DE loop.

The effective correlation time for internal motions, τ_e, in Hck SH2, was generally smaller than 50 ps (Figure 7B). Higher values (>50 ps) were found for R13, N25, N67, N92, S106, and five residues in the BC loop (E36−G40). Slower motions of τ_e on the time scale of 0.4−4 ns have been reported previously for a number of residues in interleukin-1β (*39*, *40*) and human type-α transforming growth factor (*41*). Furthermore, 26 residues required an exchange term, R_{ex}, for compensation of line broadening due to conformational or chemical exchange processes. Large exchange values were observed for residues R18, N67, N92, S100, and some residues in the BC loop. Finally, a two time scale model was required to fit the data for 27 residues while relaxation data for 16 residues of the free protein could not be fitted to any model. These data suggest that site-specific motions at an intermediate time scale (2−5 ns) are present across the entire domain.

Explicit consideration of rotational anisotropy for Hck SH2 resulted in only small changes for the numerical values of the relaxation parameters (*42*−*45*). Exclusion of M26 and Q82 improved the fit of the data that was adequately described by an axially symmetric model for rotational diffusion and not further improved by consideration of a fully anisotropic model. The optimum global correlation time (τ_m) was increased slightly from 6.8 ns for isotropic rotation to 7.1 ns considering an axially symmetric model (7.2 ns omitting M26 and Q82). Numerical values of the order parameter were insensitive to the orientation of the NH bond vectors relative to the long axis of the diffusion tensor for $D_{||}/D_{\perp} \approx 1.3$. Consideration of S_f^2 values ($D_{||}/D_{\perp} \approx 1.3$, $\tau_c = 7.0$ ns) between 0.30 and 0.85 and internal correlation times (τ_e) of 20 and 100 ps resulted in errors of less than 2% due to exclusion of anisotropic rotational diffusion. Neglect of rotational anisotropy had a larger effect on

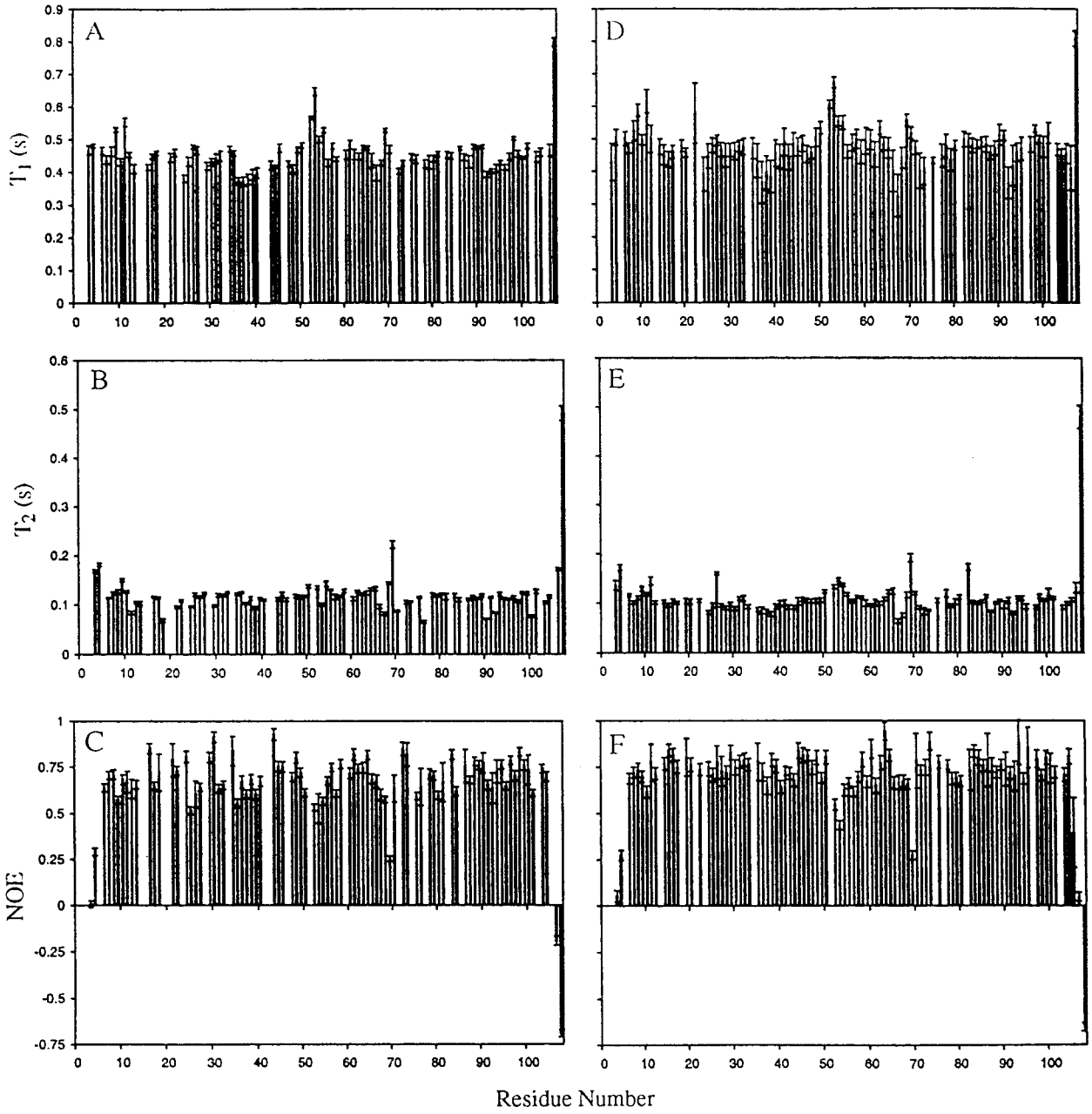

FIGURE 6: Plots of ^{15}N relaxation data as a function of residue number for the Hck SH2 domain. Panels A−C are for the free protein, and panels D−F are for the phosphopeptide-complexed protein. Measured values of spin−lattice relaxation time (T_1) are shown in panels A and D, values of spin−spin relaxation time (T_2) are shown in panels B and E, and heteronuclear NOE data are shown in panels C and F.

calculation of τ_e with even the low anisotropy of the Hck SH2 domain capable of inducing maximal errors of 20% in these values.

Backbone Dynamics of Complexed Hck SH2. The ^{15}N and ^{1}H resonances of the backbone amides for most residues of the Hck SH2 domain were assigned from a series of titration experiments with the peptide AcNH-EPQpYEEIPIYL-COOH (*3*). The resonances for several residues decreased in intensity in the ^{1}H-^{15}N HSQC spectrum during the course of the titration and became apparent later in the titration at a different chemical shift. These results indicate that the exchange of this phosphopeptide between the free and complexed Hck SH2 domain is intermediate on the NMR time scale. Assignment of the backbone resonances for these residues was accomplished using HNHA and NOESY−HSQC experiments. The HNHA experiment identifies correlations between intraresidue amide protons and α protons while the NOESY−HSQC spectrum correlates chemical shifts of amide protons with both the intraresidue alpha protons and the α protons in the preceding residue. The combined use of these two experiments allowed all the cross-peaks in the ^{15}N HSQC spectrum for Hck SH2 to be assigned (Figure 2).

The relaxation parameters for the complexed protein are shown in Figure 6, panels D−F. For most residues, the ^{15}N T_1, T_2, and NOE values lie in the ranges 0.45−0.55 s, 90−110 ms, and 0.6−0.82, respectively (Figure 6, panels D−F). In general, the ^{15}N T_1 is slightly longer and T_2 slightly shorter for the complexed protein than was observed for the same residue in the free protein. Only one residue at the C-terminus gave a negative NOE.

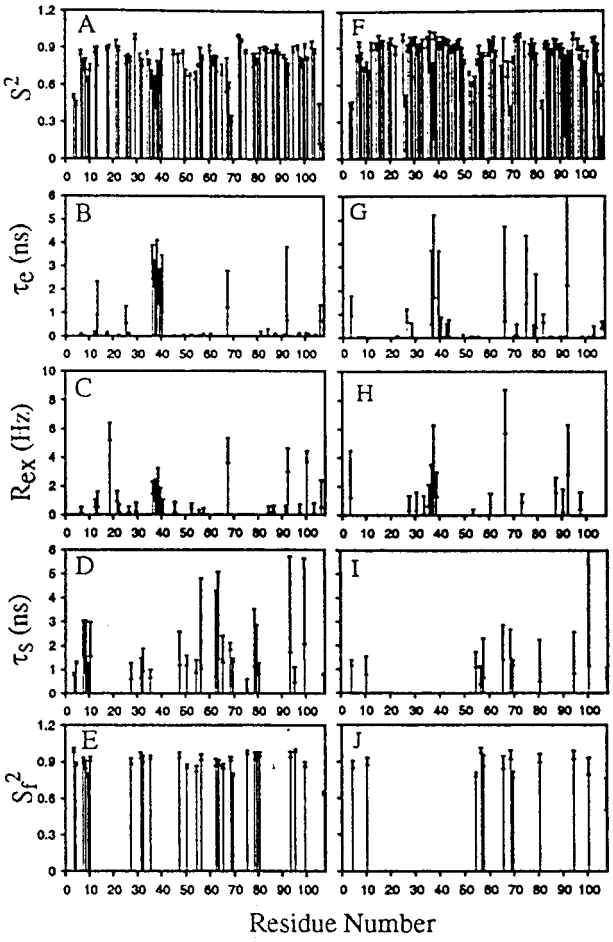

FIGURE 7: Plots of the optimized model-free and extended model-free parameters as a function of residue number for the Hck SH2 domain. Panels A−E are for the free protein, and panels F−J are for the phosphopeptide-complexed protein. Optimized values of the generalized order parameter (S^2) are shown in panels A and F, values of effective correlation time (τ_e) are shown in panels B and G, exchange parameters (R_{ex}) are shown in panels C and H while values of the effective correlation time for internal motions on a slow time scale (τ_s) are shown in panels D and I and values of the generalized order parameter for fast motion (S_f^2) are shown in panels E and J.

Table 1: Summary of Spectral Density Models Used to Fit T_1, T_2, and NOE Data for the Free and Phosphopeptide-Complexed Hck SH2 Domain

model parameters	free	complexed
S^2	7	35
S^2 and τ_e	9	26
S^2 and R_{ex}	5	10
S^2, τ_e, and R_{ex}	21	6
S_s2, S_f2, and τ_s	27	12
not fit	16	4
total	85	93

The optimum global τ_m for the complexed protein was determined to be 7.6 ns using the same procedure as described above for the free protein. This value was used to calculate the extended model free parameters for the complexed protein (Figure 7, panels F−J). Several residues have lower than average order parameters, suggesting that these segments of the protein are more mobile than the overall backbone. Large effective correlation times τ_e (>50 ps) were also found for several residues located in the loop regions or at the end of the secondary structure regions, a result similar to interleukin-1β (*39*, *40*) and human type-α transforming growth factor (*41*).

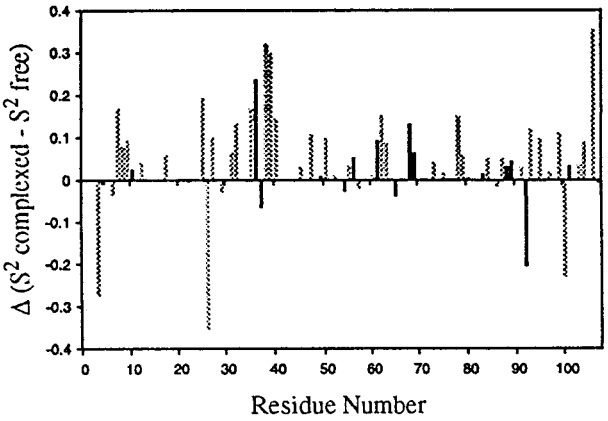

FIGURE 8: Differences between the generalized order parameters (S^2) for the free and phosphopeptide-complexed Hck SH2 domain. Only the residues whose relaxation parameters were determined for both forms were included in this plot. Solid lines indicate that the same model was used to fit the relaxation data for both the free and complexed Hck SH2 domain, whereas gray lines indicate different models were used.

Backbone Dynamics of Free and Complexed Hck SH2. The spectral density models used to fit the free and complexed Hck SH2 domain are summarized in Table 1. Relaxation data for most residues in the phosphopeptide complexed Hck SH2 are fit well using a simple model, whereas either an exchange term or a two time-scale model is required to fit most of the residues in free Hck SH2. The differences between the order parameters (S^2) for the free and the complexed states of Hck SH2 are shown in Figure 8. Most residues, especially those implicated in peptide binding, exhibit increased order parameters in the complexed protein relative to the free state. The larger numerical values for order parameters calculated for several residues in the phosphopeptide complex of Hck SH2 relative to the free domain probably do not result from different models that were used to fit the data since the same trends were evident for residues fit using identical models. Explicit consideration of anisotropic contributions to relaxation processes also could not account for the systematically larger values for order parameters calculated for the complexed form of Hck SH2 relative to the free domain since the relatively low degree of anisotropy for Hck SH2 induces a maximal deviation of only a few percent in the order parameters (see above; *45*) (Figure 8).

The results obtained are consistent with complexation of Hck SH2 by the high affinity phosphopeptide ligand resulting in adoption of a single binding mode with decreased internal motion relative to the uncomplexed state. This observation is different from that reported for the PLCγ SH2 domain for which order parameters for a large number of residues decreased upon phosphopeptide binding, apparently as a consequence of multiple binding conformations (*29*). A small number of residues not involved in peptide binding (T3, M26, N92, and S100) in the complexed Hck SH2 domain, however, displayed decreased order parameters relative to the values in the free state, an indication of increased local motions may occur for these residues.

Conclusions. We have determined the diffusion coefficients and backbone dynamics of the Hck SH2 domain both in the free and in the phosphopeptide-complexed forms. Both the free and the complexed forms of Hck SH2 domain undergo self-association at high concentrations, resulting in dimerization and formation of higher order aggregates. These results suggest that residues outside the phosphopeptide-binding site of Hck SH2 might be involved in self-association, probably through charged interactions. While limited self-association of the free form of PLC-γ SH2 has been reported, self-association of the complexed form of an SH2 domain has not, to our knowledge, been previously observed (*29*).

The observation that the numerical values for the order parameters calculated for residues in the complexed form of Hck SH2 are systematically larger than those calculated for the same residues in the free domain is, perhaps, more significant for the biological activity of Hck in vivo. These larger numerical values for order parameters in the phosphopeptide complex indicates motion on the picosecond time scale of the NH bond vectors is restricted upon complexation. This restriction in fast (ps) motion in the peptide backbone that accompanies ligand binding can be interpreted in terms of a change in entropy due to complexation. Numerical estimation of the magnitude of the entropic changes that accompany phosphopeptide binding to Hck SH2 using the assumptions described by Kay et al. reveals the entropic penalty for ligand binding for those residues experiencing the largest changes in order parameter are about 2.0 J/mol K (*46*−*48*). These changes, while individually quite small, are widespread across the entire domain (see Figure 8) and concertedly may influence the thermodynamic favorability of ligand binding. Thus, intra- or intermolecular complexation of Hck SH2 with a phosphotyrosine-containing ligand carries with it an entropic penalty for the increased order of the NH bond vectors in the SH2 peptide backbone. Conversely, phosphopeptide release from Hck SH2 is entropically favored by the decrease in order of the backbone for the domain. Our results are consistent with changes in the dynamic motion of the Hck SH2 backbone playing a significant role in regulation of Hck kinase activity by providing a thermodynamic driving force for the release of phophotyrosine-containing ligands.

A recent study by Fesik and co-workers also revealed similar changes in dynamic behavior of a protein upon binding a phosphopeptide, as were observed in the present study (*49*). In the latter study, the insulin receptor substrate 1 phosphotyrosine-binding domain showed increased order parameters upon binding an IL-4 receptor phosphopeptide. These similar results in different systems suggest entropic increases in proteins accompanying phosphopeptide release may be a general phenomenon. Complete understanding of the thermodynamics of molecular recognition processes important for signal transduction is required to understand these important natural phenomena and to intervene rationally in disease states characterized by unwarranted signaling processes (*47*).

ACKNOWLEDGMENT

Special thanks to Nico Tjandra for performing the anistropic relaxation analysis. We also thank Mr. David Babcook for technical assistance and gratefully acknowledge Professor Lewis E. Kay and Dr. Neil A. Farrow for providing the extended model-free program.

SUPPORTING INFORMATION AVAILABLE

A description of the processing and analysis of the relaxation data (*50*−*55*) (4 pages). Ordering information is available on any current masthead page.

REFERENCES

1. Pawson, T., and Schlessinger, J. (1993) *Curr. Biol. 3*, 434−442.
2. Cohen, G. B., Ren, R., and Baltimore, D. (1995) *Cell 80*, 237−248.
3. Waksman, G., Shoelson, S. E., Pant, N., Cowburn, D., and Kuriyan, J. (1993) *Cell 72*, 779−790.
4. Nada, S., Okada, M., MacAuley, A., Cooper, J. A., and Nakagawa, H. (1991) *Nature* 51, 69−72.
5. Xu, W., Harrison, S. C., and Eck, M. J. (1997) *Nature 385*, 595−602.
6. Sicheri, F., Moarefi, I., and Kuriyan, J. (1997) *Nature 385*, 602−609.
7. Moarefi, I., LaFevre-Bernt, M., Sicheri, F., Huse, M., Lee, C.-H., Kuriyan, J., and Miller, W. T. (1997) *Nature* 385, 650−653.
8. Parsons, J. T., and Parsons, S. (1997) *Curr. Opin. Cell. Biol. 9*, 187−192.
9. Briggs, S. D., Sharkey, M., Stevenson, M., and Smithgall, T. E. (1997) *J. Biol. Chem. 272*, 17899−17902.
10. Ziegler, S. F., Marth, J. D., Lewis, D. B., and Perlmutter, R. M. (1987) *Mol. Cell. Biol. 7*, 2276−2285.
11. Quintrell, N., Lebo, R., Varmus, H., Bishop, J. M., Pettenati, M. J., Le Beau, M. M., and Diaz, M. O. (1987) *Mol. Cell. Biol. 7*, 2267−2275.
12. Holtzman, D. A., Cook, W. D., and Dunn, A. R. (1987) *Proc. Natl. Acad. Sci. U.S.A.* 84, 8325−8329.
13. Klemsz, M. J., McKercher, S. R., Maki, R. A. (1987) *Nucleic Acids Res. 15*, 9600−9602.
14. English, B. K., Ihle, J. N., Myracle, A., and Yi, T. (1993) *J. Exp. Med. 178*, 1017−1022.
15. Ziegler, S. F., Wilson, C. B., and Perlmutter, R. M. (1988) *J. Exp. Med. 168*, 1801−1810.
16. Boulet, I., Ralph, S., Stanley, E., Lock, P., Dunn, A. R., Green, S. P., and Phillips, W. A. (1992) *Oncogene 7*, 703−710.
17. Ghazizadeh, S., Bolen, J. B., and Fleit, H. B. (1994) *J. Biol. Chem. 269*, 8878−8884.
18. Wang, A. V. T., Scholl, P. R., and Geha, R. S. (1994) *J. Exp. Med. 180*, 1165−1170.
19. Durden, D. L., Kim, H. M., Calore, B., and Liu, Y. (1995) *J. Immunol. 154*, 4039−4047.
20. Lowell, C. A., Fumagalli, L., and Berton, G. (1996) *J. Cell Biol. 133*, 895−910.
21. Saksela, K., Cheng, G., Baltimore, D. (1995) *EMBO J. 14*, 484−491.
22. Lee, C.-H., Leung, B., Lemmon, M. A., Zheng, J., Cowburn, D., Kuriyan, J., and Saksela, K. (1995) *EMBO J. 14*, 5006−5015.
23. Lee, C.-H., Saksela, K., Mirza, U. A., Chait, B. T. and Kuriyan, J. (1996) *Cell 85*, 931−942.
24. Nicholson, L. K., Kay, L. E., Baldisseri, D. M., Arango, J., Young, P. E., Bax, A., and Torchia, D. A. (1992) *Biochemistry 31*, 5253−5263.
25. Akke, M., Skelton, N. J., Kordel, J., Palmer, A. G., III, and Chazin, W. J. (1993) *Biochemstry 32*, 9832−9844.
26. Cheng, J.-W., Lepre, C. L., Chambers, S. P., Fulghum, J. R., Thomson, J. A., and Moore, J. M. (1993) *Biochemistry 32*, 9000−9010.
27. Cheng, J.-W., Lepre, C. L., and Moore, J. M. (1994) *Biochemistry 33*, 4093−4100.
28. Fushman, D., Weisemann, R., Thüring, H., and Rüterjans, H. (1994) *J. Biomol. NMR 4*, 61−78.

29. Farrow, N. A., Muhandiram, R., Singer, A. U., Pasal, S. M., Kay, C. M., Gish, G., Shoelson, S. E., Pawson, T., Forman-Kay, J. D., and Kay, L. E. (1994) *Biochemistry 33*, 5984−6003.
30. Yu, L., Zhu, C.-X., Tse-Dinh, Y. C., and Fesik, S. W. (1996) *Biochemstry 35*, 9661−9666.
31. Zhang, W., Smithgall, T. E., and Gmeiner, W. H. (1997) *J. Biomol. NMR 10*, 263−272.
32. Zhang, W., Smithgall, T. E., and Gmeiner, W. H. (1997) *FEBS Lett. 406*, 131−135.
33. Wu, D., Chen, A., and Johnson, C. S., Jr. (1995) *J. Magn. Reson., Ser. A 115*, 260−264.
34. Smallcombe, S. H., Patt, S. L., and Keifer, P. A. (1995) *J. Magn. Reson., Ser. A 117*, 295−303.
35. Kay, L. E., Torchia, D. A., and Bax, A. (1989) *Biochemistry 28*, 8972−8979.
36. Payne, G., Shoelson, S. E., Gish, G. D., Pawson, T., and Walsh, C. T. (1993) *Proc. Natl. Acad. Sci. U.S.A. 90*, 4902−4906.
37. Ilyina, E., Roongta, V., Pan, H., Woodward, C., and Mayo, K. H. (1997) *Biochemistry 36*, 3383−3388.
38. Fushman, D., Cahill, S., and Cowburn, D. (1997) *J. Mol. Biol. 266*, 173−194.
39. Clore, G. M., Szabo, A., Bax, A., Kay, L. E., Driscoll, P. C., and Gronenborn, A. M. (1990) *J. Am. Chem. Soc. 112*, 4989−4991.
40. Clore, G. M., Driscoll, P. C., Wingfield, P. T., and Gronenborn, A. M. (1990) *Biochemistry 29*, 7387−7401.
41. Li, Y.-C., and Montelione, G. T. (1995) *Biochemstry 34*, 2408−2423.
42. Tjandra, N., Garrett, D. S., Groneborn, A. M., Bax, A., and Clore, G. M. (1997*) Nat. Struct. Biol. 4*, 443−449.
43. Tjandra, N., Omichinski, J. G., Groneborn, A. M., Clore, G. M., and Bax, A. (1997*) Nat. Struct. Biol. 4*, 732−738.
44. Bax, A., and Tjandra, N. (1997) *Nat. Struct. Biol. 4*, 254−256.
45. Tjandra, N., Wingfield, P., Stahl, S., and Bax, A. (1996) *J. Biomol. NMR 8*, 273−284.
46. Yang, D., and Kay, L. E. (1996) *J. Mol. Biol. 263*, 369−382.
47. Kay, L. E. (1997) *Biochem. Cell. Biol. 75*, 1−15.
48. Akke, M., Bruschweiller, R., and Palmer, A. G., III (1993) *J. Am. Chem. Soc. 115*, 9832−9833.
49. Olejniczak, E. T., Zhou, M. M., and Fesik, S. W. (1997) *Biochemistry 36*, 4118−4124.
50. Palmer, A. G., III, Rance, M., and Wright, P. E. (1991) *J. Am. Chem. Soc. 113*, 4371−4380.
51. Abragam, A. (1961) *Principles of Nuclear Magnetism*, Clarendon Press, Oxford.
52. Mandel, A. M., Akke, M., and Palmer, A. G., III (1991) *J. Mol. Biol. 246*, 144−163.
53. Hiyama, Y., Niu, C.-H., Silverton, J. V., Bavoso, A., and Torchia, D. A. (1988*) J. Am. Chem. Soc. 110*, 2378−2383.
54. Lipari, G. and Szabo, A. (1982) *J. Am. Chem. Soc. 104*, 4546−4559.
55. Lipari, G. and Szabo, A. (1982) *J. Am. Chem. Soc. 104*, 4559−4570.
56. Kraulis, P. (1991) *J. Appl. Crystallogr. 24*, 946−950.
57. Koradi, R., Billeter, M., and Wüthrich, K. (1996) *J. Mol. Graphics 14*, 51−55.

BI972077E